

The test for suppressed dynamical friction in a constant density core of dwarf galaxies

Shigeki Inoue^{1*}

¹*Astronomical Institute, Tohoku University, Sendai 980-8578, Japan*

2009 January 29

ABSTRACT

The dynamical friction problem is a long-standing dilemma about globular clusters (hereafter, GCs) belonging to dwarf galaxies. GCs are strongly affected by dynamical friction in dwarf galaxies, and are presumed to fall into the galactic center. But, GCs do exist in dwarf galaxies generally. A solution of the problem has been proposed. If dwarf galaxies have a core dark matter halo which has constant density distribution in its center, the effect of dynamical friction will be weakened considerably, and GCs should be able to survive beyond the age of the universe. Then, the solution argued that, in a cored dark halo, the suppression of dynamical friction is caused by a new equilibrium state constructed by the interaction between the halo and the GC, in which a part of the halo rotates along with the GC (co-rotating state). In this study, I tested whether the solution is reasonable and reconsidered why a constant density, core halo suppresses dynamical friction, by means of N-body simulations. As a result, I conclude that the true mechanism of suppressed dynamical friction is not the co-rotating state, although a core halo can actually suppress dynamical friction on GCs significantly.

Key words: methods: N-body simulations – galaxies: dwarf – galaxies: kinematics and dynamics – galaxies: star clusters – galaxies: structure.

1 INTRODUCTION

The world we live in is a hierarchical universe, in which galaxies are made by a myriad of merging events. A Large-scale numerical simulation based on the Cold Dark Matter (CDM) theory has been operated as a greatly declarative method for the hierarchical scenario. It indicated that the structure of the universe develops from the small dark matter clumps which collapsed first, and result in the formation of large, massive dark matter halos of galaxies like our Milky Way or clusters of galaxies. In such a formation history, it is appropriate to consider that dwarf galaxies are fundamental 'building-blocks' and survivors expected to be the oldest structures of the universe. In this context, dwarf galaxies are believed to have important clues in understanding the hierarchical universe.

In this paper, I will discuss the dynamical friction problem which refers to orbital motion of GCs in dwarf galaxies. The drag force of dynamical friction is negligibly weak for the GCs in the Milky Way. In contrast, it operates strongly in small systems like dwarf galaxies (see chap. 8 of Binney & Tremaine 2008). Thus, the GCs in dwarfs are presumed to lose their orbital energy and fall into the galac-

tic center by strong friction force from the dark matter halo. According to results of both analytical and numerical studies, the timescale for a GC to fall into the center is of the order of $\sim 1Gyr$ (Tremaine 1976; Hernandez & Gilmore 1998; Oh et al. 2000; Vesperini 2000, 2001; Sánchez-Salcedo et al. 2006; Goerdt et al. 2006). But, even in the present universe, these GCs still do exist and keep their orbital motions. For example, the *Fornax* dSph galaxy has five GCs which are metal poor and as old as the universe, thus resembling the GCs of Milky Way (Buonanno et al. 1998, 1999; Strader et al. 2003; Greco et al. 2007).

However, by an analytical approach, Hernandez & Gilmore (1998) have discovered that the effect of dynamical friction is considerably weakened in a King model dark matter halo which has constant density distribution in the center, and the orbital motion of a GC can be sustained beyond the age of the universe. As for a cuspy halo (NFW profile or singular isothermal sphere), a GC is sucked into the galactic center by dynamical friction (see the fig.2 of Goerdt et al. (2006)). But, the analytical approach of Hernandez & Gilmore (1998) was constructed on the Chandrasekhar dynamical friction formula (Chandrasekhar 1943); hence, it cannot take account of velocity anisotropy of the field particles, because the formula is based on the assumption of isotropic

* E-mail:inoue@astr.tohoku.ac.jp

velocity state. On the other hand, by N-body simulations, Goerd et al. (2006) and Read et al. (2006) (hereafter, R06) numerically confirmed that the orbital shrinkage of a GC stops in a core region of halos. However, R06 concluded that an important key to this suppressed dynamical friction is a ‘co-rotating state’ between a GC and a part of dark matter halo. They argued that a part of halo particles in the constant density core begin to rotate with the GC which fell into the core region, and thus the halo constructs a new equilibrium state including the GC. The authors of R06 suggested that the dynamical friction ceases under this equilibrium; hence, the GC could survive beyond the age of the universe. Goerd et al. (2006) and R06 proposed that these results don’t depend on the mass of a GC, the orbital parameters (circular or elliptical orbit) of a GC, or the size of core structure of a halo (core radius).

However, the conclusions of these studies, Hernandez & Gilmore (1998) and R06, imply a discrepancy between them. As noted above, the approach of Hernandez & Gilmore (1998) is based on the Chandrasekhar formulation, and cannot take into account velocity anisotropy. But, contrary to Hernandez & Gilmore (1998), R06 concluded that the mechanism of suppressed dynamical friction is the very anisotropy in the velocity state: the co-rotating state. My aim in this paper is to assess the authenticity of the co-rotating state proposed by R06, as the mechanism of the suppressed dynamical friction.

Moreover, although the result of R06 appears to be convincing, the new equilibrium, the co-rotating state, will be vulnerable to perturbation on the GC as discussed below. Once the GC orbit is perturbed and the orbital plane inclined, the co-rotating equilibrium state will be broken easily. This means that the system is no longer equilibrium, and the dynamical friction force on the GC will be rejuvenated. R06 have also mentioned this fragile nature of the co-rotating equilibrium state. In R06 they studied single GC cases only. But, of course, real dwarf galaxies don’t necessarily have only one GC, but several or more (Durrell et al. 1996; Miller et al. 1998; Lotz et al. 2004). It can be expected that the GCs in a dwarf will be perturbed by gravity from the other GCs. Then, I infer that some GCs would fall into the galactic center by such orbital perturbation and may merge and form a stellar nucleus cluster at the galactic center (Miocchi et al. 2006; Capuzzo-Dolcetta & Miocchi 2008). Actually, some dwarf galaxies have a nucleus stellar cluster at their center, and some observational researchers have discussed that some of these nuclei may be remnants of GCs (Miller et al. 1998; Lotz et al. 2004). I conducted N-body simulations to examine whether the GCs in dwarfs fall into the galactic center by perturbation from the other GCs, even in the case of cored halo structure, or if dynamical friction is indeed suppressed by a cored dark halo even under frequent perturbation on GCs.

This paper is organized as follows: in the next section, I will explain my simulation method and models in detail; in the 3rd section I will show my simulation results and their analysis; I will discuss my results, comparing them with preceding studies, and give my conclusion in the 4th section.

2 THE SIMULATIONS

My simulational settings are almost the same as the N-body simulation of R06. There are a few differences between R06 and mine regarding the models of a halo and GC.

The simulations are pure N-body simulations (no gas component). I use a Barnes-Hut modified tree-code (Barnes & Hut 1986; Barnes 1990) in order to lighten the heavy burden of gravitational force calculation, setting an open angle of $\theta = 0.5$. A special-purpose calculator for collisionless N-body simulations, GRAPE-7 model 600, is used with the tree algorithm to accelerate gravity calculation (Makino 1991). The total number of timesteps is 11841 for the whole of a simulated period which corresponds to 10 Gyr in real timescale. It takes roughly a half month to finish each simulation.

2.1 The setting of halo model

To imitate R06, I adopt the same spherical density distribution:

$$\rho(r) = \frac{\rho_0}{(r/r_s)^\gamma [1 + (r/r_s)^\alpha]^{(\beta-\gamma)/\alpha}} \quad ; \quad r < r_{vir} \quad (1)$$

with $\alpha = 1.5$, $\beta = 3.0$, $\gamma = 0.0$. The density in the core ρ_0 is $0.10M_\odot pc^{-3}$. The scale radius r_s is set to $0.91kpc$. The density is nearly constant at the center within 200-300 pc, which defines the core region. The virial mass is $2.0 \times 10^9 M_\odot$. I add an exponentially decaying envelope to prevent instability at the outer region caused by an artificial cut-off radius r_{vir} (Springel & White 1999). Velocity dispersion is given by the solution of Jeans equations, as a function of radius,

$$\sigma_r^2(r) = \frac{1}{r^{2\beta}\rho(r)} \int_r^\infty dr' r'^{2\beta} \rho(r') \frac{d\Phi}{dr'}, \quad (2)$$

where β is the anisotropy parameter. Although the effect of dynamical friction is sensitive to the velocity distribution of the field particles, isotropic velocity state is supposed to be reasonable in inner region of dwarf halos (Mashchenko et al. 2008). In this paper, I assume the isotropic velocity state in the halo, setting $\beta = 0$ ($\sigma_r = \sigma_\theta = \sigma_\phi$). With this assumption, Eq.2 reduces to

$$\sigma^2(r) = \frac{1}{\rho(r)} \int_r^\infty dr' \rho(r') \frac{d\Phi}{dr'}. \quad (3)$$

The velocity distribution is decided by local Maxwellian approximation,

$$F(v, r) = 4\pi \left(\frac{1}{2\pi\sigma^2} \right)^{3/2} v^2 \exp\left(-\frac{v^2}{2\sigma^2}\right), \quad (4)$$

where $F(v, r)$ is the probability distribution function of velocity (Hernquist 1993). Eq.4 is normalized so that $\int_0^\infty F(v, r) dv = 1$.

Like R06 and Goerd et al. (2006), I adopt a three-shell model (Zemp et al. 2008), which consists of finer grained particles in inner shell regions and coarser particles in outer shell regions. This technique enables it to reduce computational run-time, and resolve much smaller scales in the inner region. But, this multi-shell model inevitably admits a number of heavier particles coming from the outer shells into the inner region and may induce two-body relaxation between

these different mass particles. To avoid such an unfavorable artificial effect, I refine particles in the outer shells depending on their orbit. From the initial position and velocity, I can calculate the pericenter distance of a specific particle in smooth potential given by the density profile, Eq.1. By the pericenter distance, I detect the heavier particles which are supposed to intrude into the inner region which consists of finer grained particles. These intruding particles are divided into a set of finer grained particles. The new particles will have the same radial velocity component as the original particle but a new random tangential component of the same magnitude as the original one. The divided particles are randomly placed on a sphere whose radius is the same as the initial galactocentric distance of the original particle. For a simple explanation, let's suppose that the halo consists of shells A, B and C, from inner to outer shell. The shells A, B and C consists of particles which have the mass of m_A , m_B and m_C , respectively ($m_A < m_B < m_C$). For example, if a certain particle which has the mass of m_C and initial position in the shell C intrudes into the shell A, the particle will be divided into a set of new particles which have the mass of m_A , and the number of the new particles will be m_C/m_A (for detail, see Zemp et al. 2008); therefore, not all particles in a outer shell have a uniform mass resolution, but two-body relaxation can be minimized in the inner most region.

Specifically, the particle masses are $m_A = 17.8M_\odot$, $m_B = 356M_\odot$ and $m_C = 7118M_\odot$. The inner most region, the shell A, is within $300pc$ (to be accurate, the shell A is not a shell, but a sphere). The shell B, the middle shell, is the region from $300 - 1100pc$. The shell C, the outer most shell, is the entire region of outside of the shell B. In the simulations of R06 or Goerdt et al. (2006), they have been missing this particle-dividing step; therefore, at this point my simulations have an improvement over the preceding studies. After carrying out this step, the number of particles is 8.31×10^6 in total. The softening lengths of the particles, m_A , m_B and m_C , are 3, 8 and 22 pc, respectively. I checked that my results were not sensitive to these values.

By analytical calculation, Sánchez-Salcedo et al. (2006) has proposed that the dynamical friction induced by the stellar component is not negligible in a cored dwarf halo. But, the purpose of this paper is to judge the co-rotating state proposed by R06, as the true mechanism of the suppressed dynamical friction. For fair comparison with the simulation of R06 in which stellar component was excluded, I don't take the effect from stellar component into account in my simulations here.

2.2 The setting of globular clusters

In my simulations, each GC is represented by a point mass with $m_{GC} = 2.0 \times 10^5 M_\odot$. The softening length is $10pc$. Just to make sure, I ran another simulation in which a GC was resolved by many particles, and confirmed that tidal disruption didn't destroy the GC. In this study, I don't consider mass-loss from a GC, merging between GCs, or dynamical heating by halo potential. Although these effects may play important roles in the case that the GCs are resolved by many particles (Fujii et al. 2006; Miocchi et al. 2006; Esquivel & Fuchs 2007; Capuzzo-Dolcetta & Miocchi

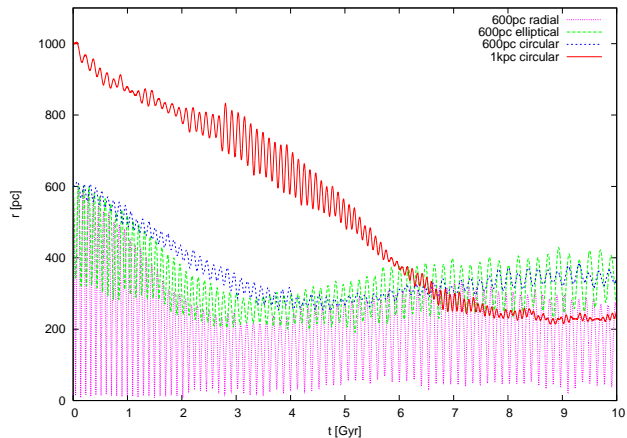


Figure 1. The results of single GC cases, each line indicates different simulation. The red line represents the time evolution of the orbital radius of the GC, which is placed on the circular orbit of radius 1.0 kpc initially. The blue, green, purple lines are for the GC initially placed on circular, elliptical and radial orbit, from radius 600 pc, respectively. The core region is inside 200-300 pc, in all simulations here.

2008), I consider the GCs as point-masses for the sake of comparison with R06 or Goerdt et al. (2006).

3 THE RESULTS

In this paper, I operate simulations for the cases of 1, 5 and 30 GCs. In single GC cases, I give the GC a set of specific orbital parameters in each case. On the other hand, in multi GC cases, I set their orbits at basically random, as detailed in the following subsections.

3.1 The single GC cases

To begin with, I conduct some single GC cases. Initial orbital radius of the GC is set to 600 pc or 1.0 kpc. The initial orbit is circular, elliptical or radial. In the case of elliptical orbit, the rotational velocity of the GC is initially set to $0.6v_{circ}$ (v_{circ} is the circular velocity on the initial orbital radius) and the radial velocity is 0. In the case of radial orbit, the GC is at rest initially. The results are indicated in Fig.1.

As shown in the figure, when a GC enters into a core region (inside 200-300 pc), the orbital shrinkage by dynamical friction stops in all cases regardless of their initial orbits. After the the cessation of dynamical friction, the orbit expands a little again. This phenomenon is called ‘kickback effect’, and a detailed investigation about the effect has been done by Goerdt et al. (2008). In my study, I don't treat this effect. These behaviors of the GC in a core (the cessation of orbital shrinkage, the kickback effect) are consistent with R06 and Goerdt et al. (2006). The mass included in the halo core is heavier than a GC by two orders, which should be enough to operate dynamical friction. Goerdt et al. (2006) has confirmed independence of suppressed dynamical friction from the size of the core region, r_s . Moreover, I find that the density profile of the halo is scarcely changed by the GC (Fig.2). The energy conservation rate of the system, $1 - E_{end}/E_{ini}$, is 6.46×10^{-3} .

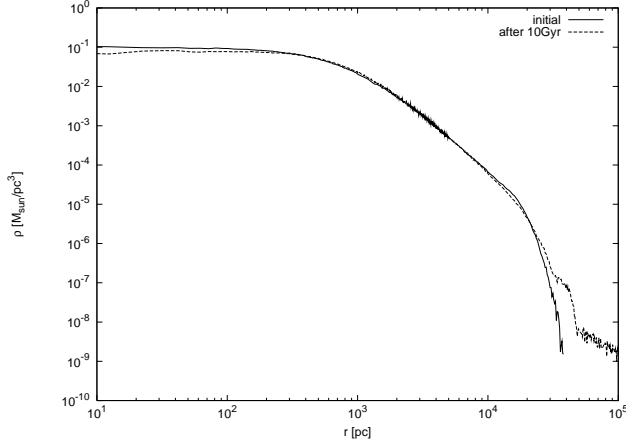


Figure 2. The density profiles in the case of the circular orbit with 1.0 kpc initial orbital radius (the red line in Fig.1). The solid line is the initial state, and the dashed line indicates the end of the simulation (after 10 Gyr). The horizontal axis is distance from the galactic center, the ordinate is mass density of the halo, $\rho[M_{\odot}/pc^3]$.

This result confirms the suppressed dynamical friction on a GC in a core halo. However, what is the cause of it? In R06, the authors have proposed that a part of halo particles in core region are made to rotate with the GC by gravitational interaction (see the fig.4 in R06). They called this dynamical state ‘co-rotating state’, and concluded it to be the mechanism to suppress the dynamical friction on the GC. I will examine whether the co-rotating state is the true mechanism or not. To identify the co-rotating state, I follow the same manner as R06. In order to visualize the velocity state of a halo, I sieve out the particles which have the radial distance $r_p = 150 - 300pc$, subject to the condition,

$$\frac{|\mathbf{J}_p \cdot \mathbf{J}_c|}{|\mathbf{J}_p||\mathbf{J}_c|} > \cos \theta, \quad (5)$$

where $\mathbf{J}_{p,c}$ means the specific angular momentum of a halo particle and the GC, respectively. A criterion parameter θ is set to 10° , which is the same value as R06. Because the halo potential is spherically symmetric and the GC is significantly heavier than any halo particles, the direction of \mathbf{J}_c is assumed to be constant in time. The condition, Eq.5, screens out the field particles for which the direction of angular momentum vector coincides with the direction of angular momentum vector of the GC within θ . Fig.3 indicates the velocity states as a histogram of rotational velocity distribution in the case of a circular orbit for which the initial orbital radius is 1.0 kpc (the red line in Fig.1). The upper panel of Fig.3 shows the initial state, the bottom panel is for $t = 8.2Gyr$ (after the cessation of dynamical friction). As seen in the bottom panel, the co-rotating state is constructed after dynamical friction is suppressed. The velocity distribution becomes somewhat anisotropic: the fraction of pro-grade rotating particles seems to increase, whereas retrograde particles decrease. The figure is consistent with the result of R06. The over-plotted dashed lines in the histograms represent Gaussian fitting given by the minimum χ^2 method. In the bottom panel (co-rotating state), the peak height of the fitting line for pro-grade side h_+ and the retrograde side h_- is 0.0132 and 0.0106, respectively. The residual

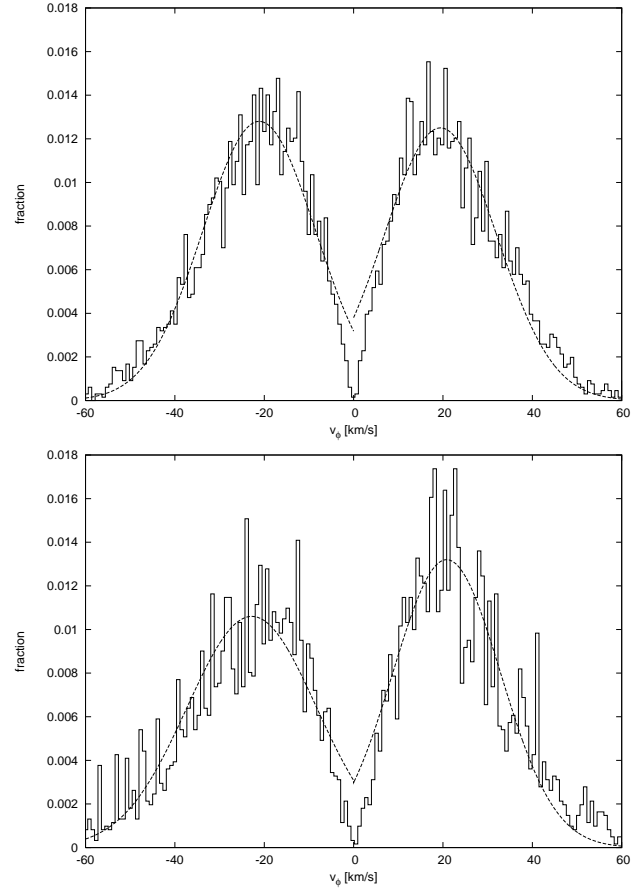


Figure 3. The histograms of the distribution of azimuthal velocity v_ϕ for the halo particles satisfying the condition of Eq.5 and $150pc < r_p < 300pc$. The vertical axis is mass fraction. The upper panel is for the initial state, and the bottom panel is for $t = 8.2Gyr$. The positive side of v_ϕ represents pro-grade rotating particles with the GC, the negative side represents retro-grade motion. The dashed lines are Gaussian fitting for each side.

fraction of these, $(h_+ - h_-)/h_-$, is 0.245. This value means that the peak of the pro-grade side is 24.5 per cent higher than that of the retrograde side. The minimum value of $|\chi|$ for the bottom panel is 0.00175, and $|\chi|/h_-$ is 0.165.

From this analysis, the existence of co-rotating state seems to be confirmed. But it may be marginal because the value of $(h_+ - h_-)/h_-$ is not significantly larger than $|\chi|/h_-$. One point to note is that the direction of \mathbf{J}_c , which is assumed to be constant, actually fluctuates due to the N-body nature of this simulation (i.e., a finite number of particles has been used) For the sake of more precise discussion, I evaluate $(h_+ - h_-)/h_-$ and $|\chi|/h_-$ for slightly different directions of \mathbf{J}_c . I re-analyze velocity states, changing the inclination of the vector \mathbf{J}_c in Eq.5 little by little. By this procedure, I draw contour maps of the value of $(h_+ - h_-)/h_-$ and $|\chi|/h_-$. The results are shown in Fig.4. As shown in the figure, co-rotating state ($(h_+ - h_-)/h_- > 0$) can be found within $\sim 10^\circ$ from the maximal direction. But, the value of $(h_+ - h_-)/h_-$ should be compared with the value of $|\chi|/h_-$. The contour map of $|\chi|/h_-$ is given in the bottom panel of Fig.4. From the map, it is found that the range of the value is $0.12 < |\chi|/h_- < 0.2$ for the entire area plotted. There-

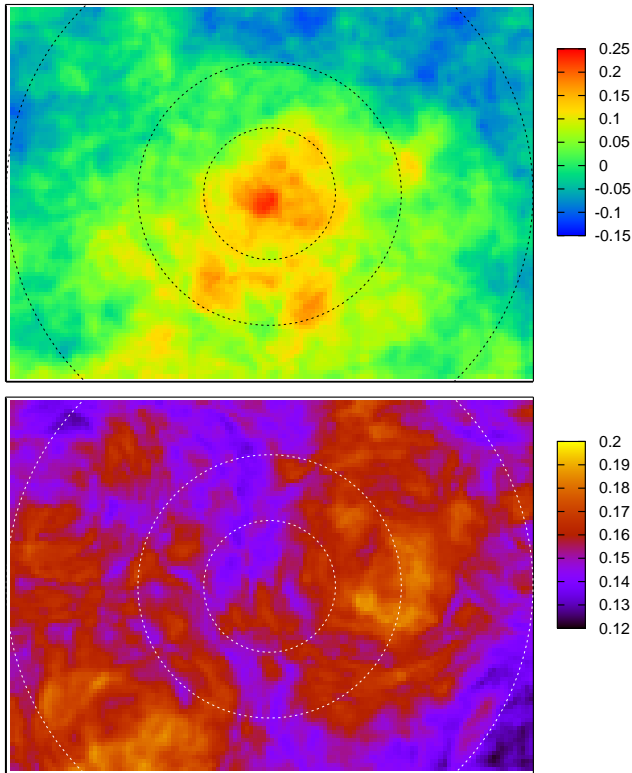


Figure 4. The contour maps of $(h_+ - h_-)/h_-$ (upper) and $|\chi|/h_-$ (bottom). The center is the direction for which the value of $(h_+ - h_-)/h_-$ is the largest (‘the maximal direction’). The dotted circles indicate 5° , 10° and 20° from this direction, from inside to outside.

fore, the value of $(h_+ - h_-)/h_-$ is almost submerged under the fitting error, $|\chi|/h_-$, in most of the area except the central region. This discussion means that the co-rotating state shown in the upper panel of Fig.4 is statistically marginal and unimportant, maybe except the central region ($\sim 3^\circ$ from the maximal direction). Such weak anisotropy couldn’t be expected to affect the dynamical friction on a GC.

Finally, I inspect the co-rotating state for the dependence on radial distance from the galactic center. So far, I’ve analyzed the co-rotating state in the radial range of $150pc < r < 300pc$. I additionally carry out the same analysis in other radial ranges, $r < 150pc$, $300pc < r < 450pc$ and $450pc < r < 600pc$, with \mathbf{J}_c unchanged. The result is indicated in Fig.5. From the figure, it can be seen that the co-rotating velocity state is constructed only in $150pc < r < 300pc$.

3.2 The 5 GCs case

From the discussion of the previous subsection, the co-rotating state not be influential in dynamical friction. Even if the co-rotating state suppresses the dynamical friction on a GC, because it would be fragile against orbital perturbation on the GC as proposed in R06, the dynamical friction would be rejuvenated by the presence of the perturbation. Actually, because real dwarf galaxies generally have some GCs (Miller et al. 1998), there are probably frequent perturbations on the GCs in real dwarfs. As an additional test

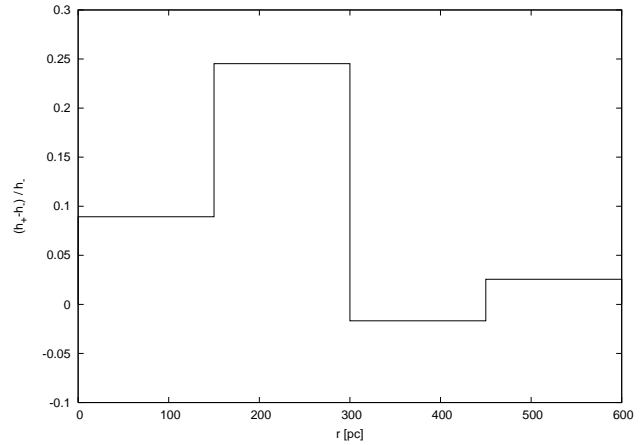


Figure 5. The radial dependence of $(h_+ - h_-)/h_-$. The width of each bin represents a radial range of the analysis. \mathbf{J}_c is fixed to the maximal direction.

for the authenticity of the co-rotating state, I perform the simulations of multi GC cases.

In this subsection, I present the result of the 5GCs case. The GCs are represented as point masses. The initial positions of the GCs are randomly determined in the radial range of $300pc < r < 2kpc$. The energy of each GC is also given randomly in the range of $E < \Phi_{2kpc}$ with a random direction of the velocity vector (Φ_{2kpc} is the potential energy of the halo at $r = 2.0kpc$). To facilitate direct comparison with single GC cases, one GC (reference GC) is placed on a circular orbit with radius 600 pc.

The results for all GCs are shown in Fig.6. The top left panel indicates the reference GC, and the other panels represent the other 4 GCs which have randomly chosen positions and velocities. As shown in Fig.6, all orbits of the GCs are frequently perturbed. From the comparison with single GC cases (Fig.1), the perturbation is expected to be caused by mutual interaction among the GCs, because the difference between these simulations is the number of GCs only. Despite these perturbations, no GCs fall into the galactic center, with all GCs surviving and keeping their orbital motions. This means that the dynamical friction is suppressed in a core region even under frequent perturbation. This implies the inconsistency with the description in R06. This result casts a doubt on the co-rotating state as the mechanism of suppressed dynamical friction, together with the analysis of the single GC case. Actually, the co-rotating state can not be found in velocity histograms of the 5GCs case.

3.3 The 30 GCs case

To confirm the result of the 5GC case, I investigate the case of 30GCs. The number of GCs in this case is somewhat too large, because the actual number of GCs in any dwarf galaxies is ~ 20 at most (Miller et al. 1998). The settings for the initial condition is basically the same as the 5GCs case: random positions and velocities are chosen except for one GC which is placed on a circular orbit with radius 600 pc (reference GC). Some simulation results of these GCs are shown in Fig.7.

As seen from Fig.7, these results are essentially the same

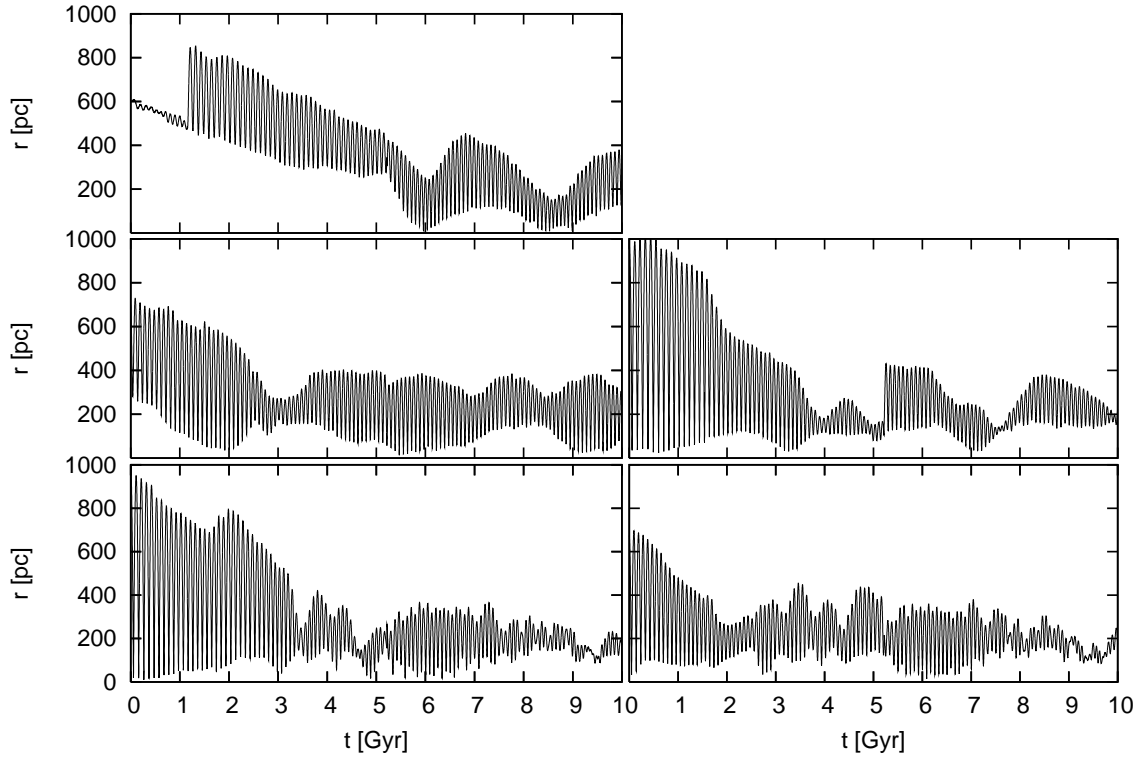


Figure 6. The simulation result of the 5 GCs case, showing the variations of orbital radius. The top left panel represents the reference GC which is initially placed on a circular orbit with a radius 600 pc. The others indicate GCs whose initial distance and velocity are randomly given.

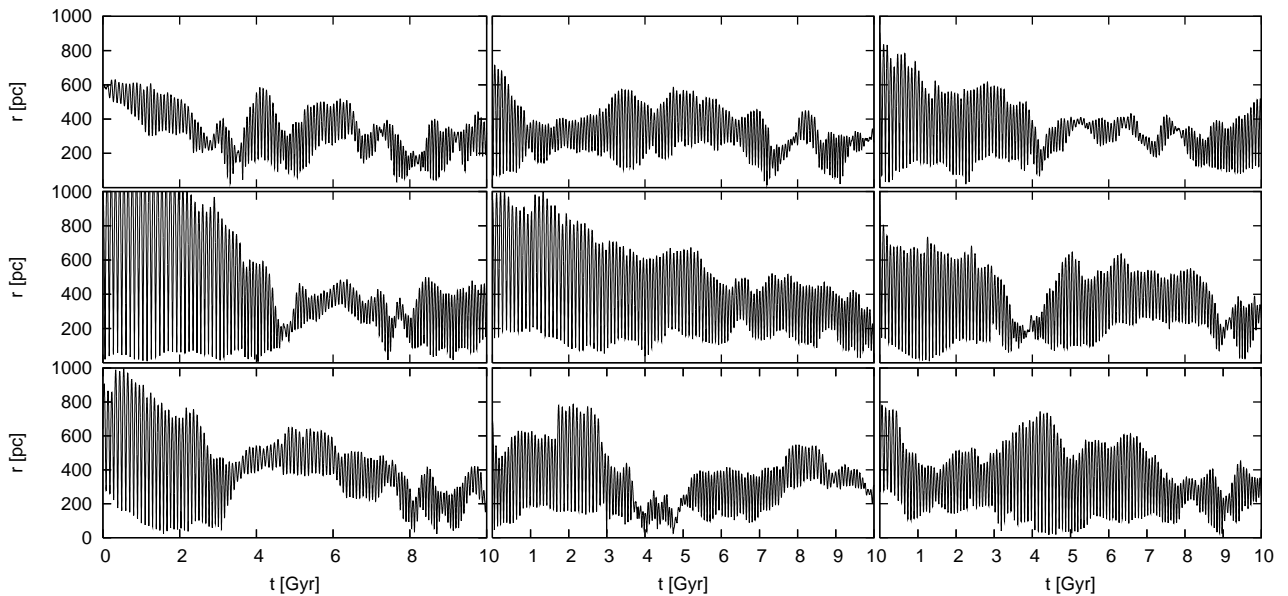


Figure 7. The same as Fig.6, but for the 30GCs case. The top left panel represents the reference GC.

as 5GCs case. Dynamical friction is suppressed in the core region despite more frequent perturbation than the 5GC case. Moreover, the co-rotation state is not confirmed in this case, and can be guessed to be broken by perturbation among numerous GCs. The result reinforces my argument.

4 DISCUSSION & CONCLUSION

My simulation results indicate as follows. On one hand, dynamical friction is indeed suppressed in a constant density core region, orbital shrinkage of a GC stops and the orbital motion is sustained. But, on the other hand, this result doesn't depend on the number of GCs. This means that the dynamical friction doesn't work in a core, even if the co-rotating state is broken by frequent perturbation. Moreover, in single GC cases the co-rotating state seems to be too marginal to affect dynamical friction. My main conclusion here is that the co-rotating state is not the true mechanism. There may be another reason why dynamical friction ceases in a constant density halo.

However, I confirmed that a cored halo structure certainly can weaken the dynamical friction force on a GC in the core region. This means that the cored structure can be the solution of the dynamical friction problem. Actually, as an observational fact, the rotation curves of Low Surface Brightness (LSB) galaxies seem to be like a solid body rotation which means a nearly constant density distribution, although CDM cosmological N-body simulations indicate cuspy density distributions (Dalcanton & Bernstein 2000; de Blok et al. 2001). Moreover, by the cosmological SPH simulation, Mashchenko et al. (2008) has discovered a dwarf galaxy which has a constant density core in the halo. They concluded that massive stars inject large amount of energy into the dark matter halo via supernova explosions, and the feedback induced by bursty star formation can turn the cuspy density distribution of the dark matter into a cored profile in the halo center. The suppressed dynamical friction would reinforce the existence of a core structure in dwarfs. If it's the case that the actual dwarfs have a core region in the center, all GCs are included within the core region of the dwarf. Thus, it can be expected that in a dwarf, the largest galactocentric distance of the GCs indicates the minimum value of the core radius. For instance, in the *Fornax* dSph, the furthest GC from the galactic center has a projected distance of $\sim 1.6kpc$ (Mackey & Gilmore 2003). The core region of the *Fornax* would be larger than $\sim 1.6kpc$.

The most fundamental examination of dynamical friction is embodied by the Chandrasekhar dynamical friction formula (Chandrasekhar 1943). However, several approximations have been dared in the derivation. Current astrophysicists realized that the formula is not always correct because of complex nonlinear effects (Jiang & Binney 2000; Hashimoto et al. 2003; Fujii et al. 2006; Kim et al. 2008). Probing the dark matter distribution of dwarfs requires more sophisticated approaches to the nature of dynamical friction.

ACKNOWLEDGMENTS

The numerical simulations reported here were carried out on GRAPE systems kindly made available by CfCA (Cen-

ter for Computational Astrophysics) at the National Astronomical Observatory of Japan. The numerical code was based on a software distributed on the website of Joshua E. Barnes (<http://ifa.hawaii.edu/~barnes/software.html>). I thank Masafumi Noguchi for his fascinating and helpful discussion.

REFERENCES

- Barnes J. 1990, *J. Comput. Phys.*, 87, 161
 Barnes J., Hut P. 1986, *Nature*, 324, 446
 Binney J., Tremaine S., 2008, *Galactic Dynamics Second Edition*. Princeton Univ. Press, Princeton
 Buonanno R., Corsi C. E., Zinn R., Pecci F. F., Hardy E., Suntzeff N. B., 1998, *ApJ*, 501, 33
 Buonanno R., Corsi C. E., Castellani M., Marconi G., Pecci F. F., Zinn R., 1999, *AJ*, 118, 1671
 Chandrasekhar S., 1943, *ApJ*, 97,255
 Capuzzo-Dolcetta R., Miocchi P., 2008, *ApJ*, 681, 1136
 Dalcanton J. J., Bernstein R. A., 2000, *AJ*, 120, 203
 de Blok W. J. G., McGaugh S. S., Bosma A., Rubin V. C., 2001, *ApJ*, 552, 23
 Durrell P. R., Harris W. E., Geisler D., Pudritz R. E., 1996, *AJ*, 112, 972
 Esquivel O., Fuchs B., 2007, *MNRAS*, 378, 1191
 Fujii M., Funato Y., Makino J., 2006, *PASJ*, 616, 642
 Goerdt T., Moore B., Read J. I., Stadel J., Zemp M., 2006, *MNRAS*, 368, 1073
 Goerdt T., Read J. I., Moore B., Stadel J., 2008, preprint (astro-ph/0806.1951)
 Greco C. et al., 2007, *ApJ*, 670, 332
 Hashimoto Y., Funato Y., Makino J., 2003, *ApJ*, 582, 196
 Hernandez X., Gilmore G., 1998, *MNRAS*, 297, 517
 Hernquist L., 1993, *ApJ*, 86, 389
 Jiang I.-G., Binney J., 2000, *MNRAS*, 314, 468
 Kim H., Kim W.-T., Sánchez-Salcedo F. J., 2008, *ApJ*, 679,33
 Lotz J. M., Miller B. W., Ferguson H. C., 2004, *ApJ*, 613, 262
 Mackey A. D., Gilmore G. F., 2003, *MNRAS*, 340,175
 Makino J. 1991, *PASJ*, 43, 621
 Mashchenko S., Wadsley J., Couchman H. M. P., 2008, *Sci*, 319, 174
 Miller B. W., Lotz J. M., Ferguson H. C., Stiavelli M., Whitmore B. C., 1998, *ApJ*, 508, 133
 Miocchi P., Capuzzo-Dolcetta R., Di Matteo P., Vicari A., 2006, *ApJ*, 644, 940
 Oh K. S., Lin D. N. C., Richer H. B., 2000, *ApJ*, 531, 727
 Read J. I., Goerdt T., Moore B., Pontzen A. P., Stadel J., 2006, *MNRAS*, 373, 1451
 Sánchez-Salcedo F. J., Reyes-Iturbide J., Hernandez X., 2006, *MNRAS*, 370, 1829
 Springel V., White D. M. 1999, *MNRAS*, 307,162
 Strader J., Brodie J. P., Forbes D. A., Beasley M. A., Huchra J. P., 2003, *AJ*, 125, 1291
 Tremaine S., 1976, *ApJ*, 203, 345
 Vesperini E., 2000, *MNRAS*, 318, 841
 Vesperini E., 2001, *MNRAS*, 322, 247
 Zemp M., Moore B., Stadel J., Carollo M., Madau P., 2008, *MNRAS*, 386, 1543